Diboronate Crosslinking: Introducing Glucose Specificity in Glucose-Responsive Dynamic-Covalent Networks

Yuanhui Xiang,[+] Sijie Xian,[+] Rachel C. Ollier, Sihan Yu, Bo Su, Irawan Pramudya, Matthew J. Webber*

University of Notre Dame, Department of Chemical & Biomolecular Engineering, Notre Dame, IN 46556 USA

*- mwebber@nd.edu

[+]- YX and SX contributed equally to this work

ABSTRACT: Dynamic-covalent motifs are increasingly used for hydrogel crosslinking, leveraging equilibrium-governed reversible bonds to prepare viscoelastic materials with dynamic properties and self-healing character. The bonding between aryl boronates and diols is one dynamic-covalent chemistry of interest. The extent of network crosslinking using this motif may be subject to competition from ambient diols such as glucose; this approach has long been explored for glucose-directed release of insulin to control diabetes. However, the majority of such work has used phenylboronic acids (PBAs) that suffer from low-affinity glucose binding, limiting material responsiveness. Moreover, many PBA chemistries also bind with higher affinity to certain non-glucose analytes like fructose and lactate than they do to glucose, limiting their specificity of sensing and therapeutic deployment. Here, dynamic-covalent hydrogels are prepared that, for the first time, use a new diboronate motif with enhanced glucose binding—and importantly improved glucose specificity—leveraging the ability of rigid diboronates to simultaneously bind two sites on a single glucose molecule. Compared to long-used PBA-based approaches, diboronate hydrogels offer more glucose-responsive insulin release that is minimally impacted by non-glucose analytes. Improved responsiveness translates to more rapid blood glucose correction in a rodent diabetes model. Accordingly, this new dynamic-covalent crosslinking chemistry is useful in realizing more sensitive and specific glucose-responsive materials.

KEYWORDS: Biomaterials, Self-Healing Materials, Drug Delivery, Materials Chemistry

INTRODUCTION

Hydrogels are a common class of biomaterials, with their network structure offering a surrogate of the natural extracellular matrix and their highly hydrated porosity enabling controlled release of encapsulated macromolecules.[1–6] The polymers used in composing hydrogels are typically hydrophilic, and once crosslinked afford a material that can imbue water in an amount many times the dry weight of the polymer itself.[7] Hydrogels can be characterized by their mode of crosslinking; chemical crosslinking entails the permanent formation of covalent crosslinks between polymer chains, while physical crosslinking arises from transient and reversible interactions or entanglements.[8,9] The mechanical properties of the bulk hydrogel materials usually follow directly from their mode of crosslinking. Covalent crosslinks commonly yield materials with higher modulus that do not flow or permanently deform under moderate strain but exhibit permanent loss of mechanical character under high strain. Conversely, physical crosslinking typically gives rise to materials with more dynamic viscoelastic behavior, enabling flow under applied strain and exhibiting self-healing character.

Dynamic-covalent chemistry encompasses a number of equilibrium-governed covalent bonds, including many classical organic reaction mechanisms.[10,11] Recently, dynamic-covalent crosslinking has gained attention for its use in the preparation of hydrogels.[12–14] When used in the context of hydrogel crosslinking, this approach enables covalent bonding interactions with dynamic exchange and finite average lifetime. Accordingly, this mode of crosslinking, in principle, affords aspects of both chemical and physical crosslinking in yielding dynamic viscoelastic materials with well-defined crosslinking interactions and excellent mechanical properties while also undergoing equilibrium-governed bond exchange

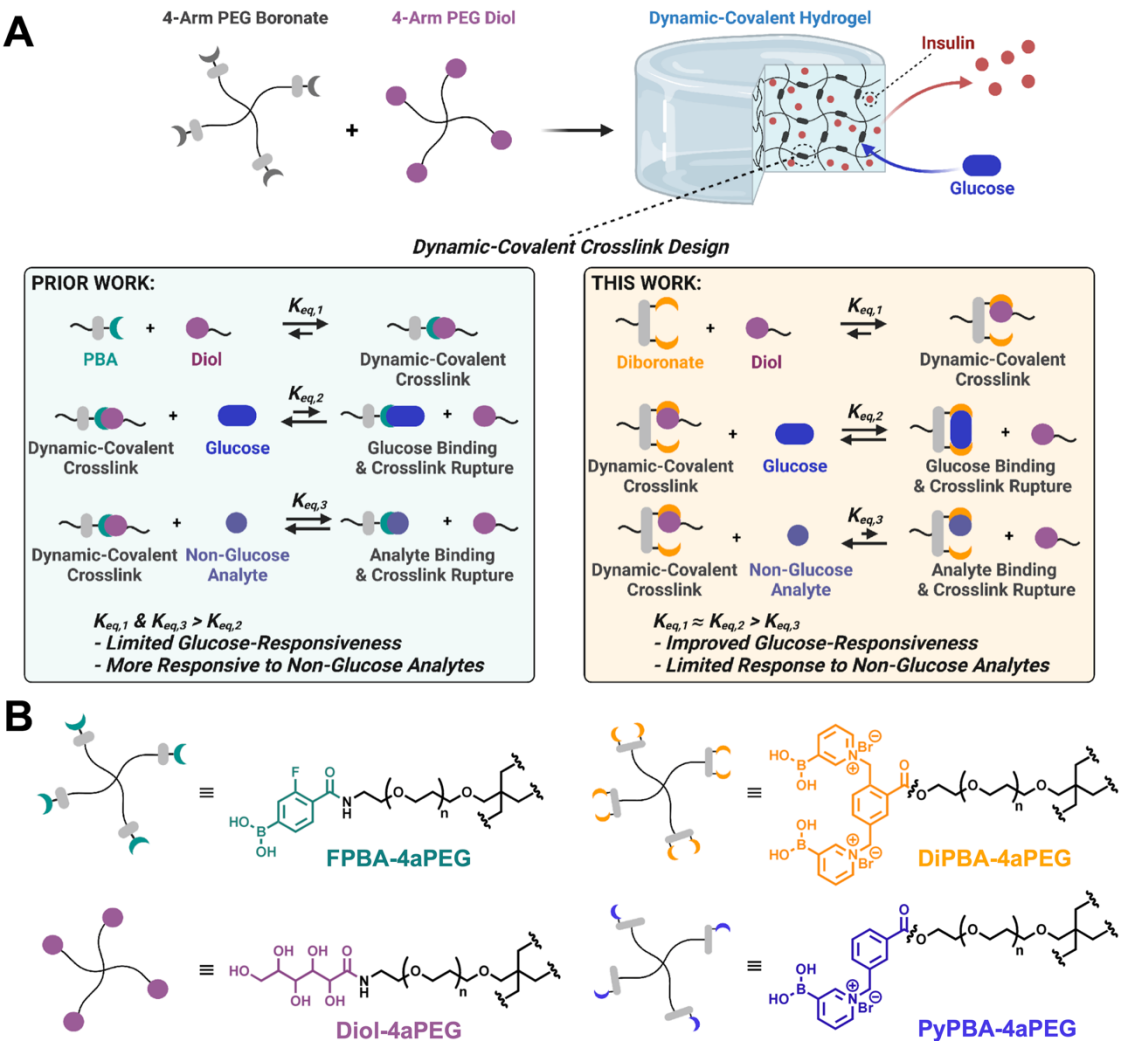

Figure 1: (**A**) Hydrogel networks are prepared from dynamic-covalent crosslinking interactions between aryl boronates and diols, each appended to a 4-arm polyethylene glycol (PEG) macromer. As these interactions are susceptible to competition from free diols such as glucose, this approach offers a route to materials for glucose-responsive delivery of insulin. However, traditional phenylboronic acids (PBAs) used thus far do not bind glucose with affinity (K_{eq}) necessary for optimal function in physiologic conditions, and also bind to non-glucose analytes such as fructose and lactate with high affinity. The present work instead explores dynamic-covalent crosslinking with a diboronate (DiPBA) group, offering high-affinity glucose binding and greater resistance to binding non-glucose analytes, with the goal of more sensitive and specific glucose-responsive function. (**B**) Chemical structures of 4-arm PEG (4aPEG) macromers used in this work, bearing a fluorine-substituted PBA (FPBA), diboronate motif (DiPBA), pyridine-PBA (PyPBA), or glucose-like diol (Diol) moiety.

that enables network restructuring and self-healing. Certain of these dynamic-covalent interactions are further modulated by competition from naturally occurring analytes, enabling their equilibrium-governed bond exchange to be integrated into stimuli-responsive platforms. One such chemistry that has been explored in this regard is dynamic-covalent bonding between phenylboronic acids (PBAs) and *cis*-1,2 or *cis*-1,3 diols.[15] In the context of drug delivery for diabetes, PBA–diol chemistry is susceptible to competition from glucose (a *cis*-1,2 diol), which in turn creates hydrogels where the extent of network crosslinking may be rendered glucose-dependent.[16]

Prior reports have described hydrogel materials crosslinked using PBA–diol interactions and explored glucose-responsive release of encapsulated macromolecules from these networks.[17–20] Rich phenomena in polymer physics have also been elucidated from ideal network platforms prepared using this chemistry.[21] At the same time, PBA chemistry presents two key drawbacks in its application for use in glucose-responsive materials. First, common diol chemistries used for polymer crosslinking have affinity for PBA significantly higher than that of glucose, which itself does not typically bind PBA with affinity sufficient for optimal function under physiological glucose concentrations. This challenge, in turn, limits glucose-responsive function of

the material. Second, the non-specific nature of the PBA–glucose interaction means these linkages are subject to interference from binding of common analytes such as fructose and lactate,[19] which actually bind with higher affinity than glucose to most PBA chemistries.[22,23] Accordingly, limited glucose-responsiveness and sensitivity to non-glucose analytes present in the body act contrary to the envisioned application of these materials for stimuli-responsive release of insulin to control blood glucose levels in diabetes (***Fig 1A***).

A dynamic-covalent crosslinking chemistry is reported here that, for the first time, leverages high-affinity and glucose-specific interactions from diboronate (DiPBA) motifs (***Fig 1A***). Inspired by work using rigid aromatic diboronates as fluorescent or electrochemical glucose sensors for their ability to simultaneously bind two distinct sites on glucose,[24–27] the present work explores the use of a novel related motif in the formation of hydrogel networks. By appending a DiPBA motif on a 4-arm polyethylene glycol (4aPEG), its mixture with a Diol-4aPEG yields dynamic and self-healing hydrogels (***Fig 1B***). These materials exhibit improved glucose-responsivity when compared to a standard PBA chemistry (FPBA) used in many prior reports, and in addition are more resistant to physiologically relevant concentrations of fructose and lactate. This design approach using motifs that bind glucose with high affinity and improved specificity furthermore offers dynamic injectable materials with improved function in encapsulation and glucose-responsive release of insulin *in vitro* and *in vivo*.

RESULTS & DISCUSSION

Diboronate Design. Previously reported diboronate glucose sensors include architectures of two phenylboronic acids attached to an aryl core *via* charged ammonium linkers.[24,27] In a variation on this approach, the DiPBA motif explored here has introduced adjacent charge *via* pyridine-based phenylboronic acid structures (***Fig 1B***). Diboronates are bidentate glucose binders, with a reported preference to bind two sites on glucose in its less abundant α-furanose form under aqueous conditions.[28,29] Besides conserving adjacent positive charge, the topology of this novel DiPBA design was also intended to afford a more rigid pocket for simultaneous glucose binding by both boronates (***Fig S1***). Details for the synthesis and molecular characterization of this novel DiPBA group, along with all other synthetic small molecules and macromers, are reported in the *Online Supporting Information*. As a control for this glucose-binding motif, a single pyridine-PBA (PyPBA) was also synthesized. DiPBA and PyPBA motifs were compared in this work to a fluorine-substituted PBA motif (FPBA) that has been routinely reported in glucose-responsive materials and therapeutic constructs.[17,30] PBA binding to glucose and related diols exhibits a known dependence on the pK_a of the boronate, with glucose binding occurring preferentially at pH values near or above the pK_a of the particular PBA used. Accordingly, the pK_a values of these three motifs were estimated by acid-base titration (***Fig S2***), and found to be pK_{a1}=4.53 and pK_{a2}=7.45 (DiPBA), 4.41 (PyPBA), and 7.32 (FPBA). These results are comparable to previously reported pK_a values for an FPBA variant (~7.2) and a PyPBA variant (~4.4).[31,32]

Molecular-Scale Binding Validation. To first quantify the affinities of binding for these different PBA motifs to glucose, related analytes, and model diols, a set of small molecules (***Fig S3***) were synthesized for isothermal titration calorimetry (ITC) studies. A number of important trends emerge from these data (***Fig 2A, Fig S4-S7***). For the DiPBA motif, its K_{eq} for binding to glucose was 1295 M^{-1}, which was 1.7 times higher than that for fructose and 29 times higher than that for lactate. By comparison, the commonly used FPBA motif had K_{eq} for glucose binding of only 8.6 M^{-1}. This FPBA chemistry, meanwhile, demonstrated affinity for fructose that was 78 times higher and affinity for lactate that was 8 times higher than was found for glucose binding. The magnitude of FPBA binding to glucose from these measurements was comparable to values previously reported for related PBA chemistries (4.6 M^{-1}), with this same prior report also noting affinity for fructose that was ~35 times higher than that for glucose.[22] Comparing the present results to published data obtained using common spectroscopic methods furthermore support the use of ITC in this present study Accordingly, concerns over low-affinity glucose-binding and poor glucose selectivity of traditional PBAs are supported by these ITC data, with both issues seemingly overcome using DiPBA chemistry. Interestingly, the PyPBA chemistry showed increased affinity for glucose (164.7 M^{-1}) compared to FPBA, while also having relatively reduced fructose and lactate binding. In addition, to explore the likely outcomes of using each of these PBA motifs in the context of dynamic-covalent networks a model diol (GdL-Diol) was prepared from reaction of glucono-δ-lactone (GdL) with benzylamine. The K_{eq} of binding for each PBA motif to this model diol were nearly identical (~$5x10^3$ M^{-1}). Moreover, ITC model fitting yielded a predicted 'n' value for diol:PBA that was nearly identical for all PBAs (*e.g.*, n=0.713 for DiPBA and n=0.851 for FPBA). Taken together, these findings confirm similar 1:1 binding stoichiometry between all three PBA chemistries studied here and the GdL-derived diol chemistry commonly used

in preparing dynamic-covalent PBA–diol networks in spite of two boronate species on the DiPBA motif.

Hydrogel Network Preparation. Once small molecules were synthesized and validated for binding using ITC, PBA-modified macromers were prepared by end-group functionalization of 10 kDa 4-arm polyethylene glycol (4aPEG, ***Fig 1B***), with the goal of realizing hydrogel networks through dynamic-covalent PBA–diol crosslinking. Briefly, DiPBA-4aPEG and PyPBA-4aPEG were synthesized *via* thiol-maleimide Michael addition between 4aPEG-SH and maleimide-modified DiPBA or PyPBA small molecules (***Fig S13-S14***). This route used high-yielding conjugation chemistry to achieve quantitative modification of macromers, simultaneously avoiding harsh alternative reaction conditions that were found to compromise stability of pyridine-based PBA motifs in preliminary efforts. The FPBA-4aPEG was synthesized *via* amide formation between 4aPEG-NH_2 and 4-carboxy-3-fluorophenylboronic acid following previously reported methods,[17] achieving quantitative functionalization here (***Fig S15***). To prepare a diol-modified macromer (Diol-4aPEG) for construction of the hydrogel network, 4aPEG-NH_2 was reacted with GdL in the presence of triethylamine as previously reported,[17] yielding a fully modified macromer here (***Fig S16***).

With modified 4aPEG macromers in hand, hydrogel networks prepared from these macromers were next evaluated. Dynamic-covalent hydrogels were formed over a range of macromer concentrations by combining equimolar Diol-4aPEG with each of the PBA-modified 4aPEGs for oscillatory rheology, first performing a strain sweep to verify the linear viscoelastic region and then performing a frequency sweep at constant strain of 3% (***Fig 2B, Fig S20***). The G′/G″ crossover is often used to estimate k_{off} for dynamically associating networks,[33,34] wherein $k_{off}=\tau_R^{-1}$. Under oscillatory deformation, only the energy that remains in bonds over the timescale of oscillation contributes to G′, and thus the G′/G″ crossover point reflects the time constant for average bond lifetime in the network. These data thus reveal highly dynamic networks, with a time constant of network relaxation (τ_R) estimated to be ~7 s for the DiPBA–diol network on the basis of the G′/G″ crossover frequency. Some differences in k_{off} are evident when comparing DiPBA (0.14 s^{-1}), FPBA (0.45 s^{-1}), and PyPBA (0.23 s^{-1}). In the terminal regime assessed at low frequency, the rate of bond reorganization

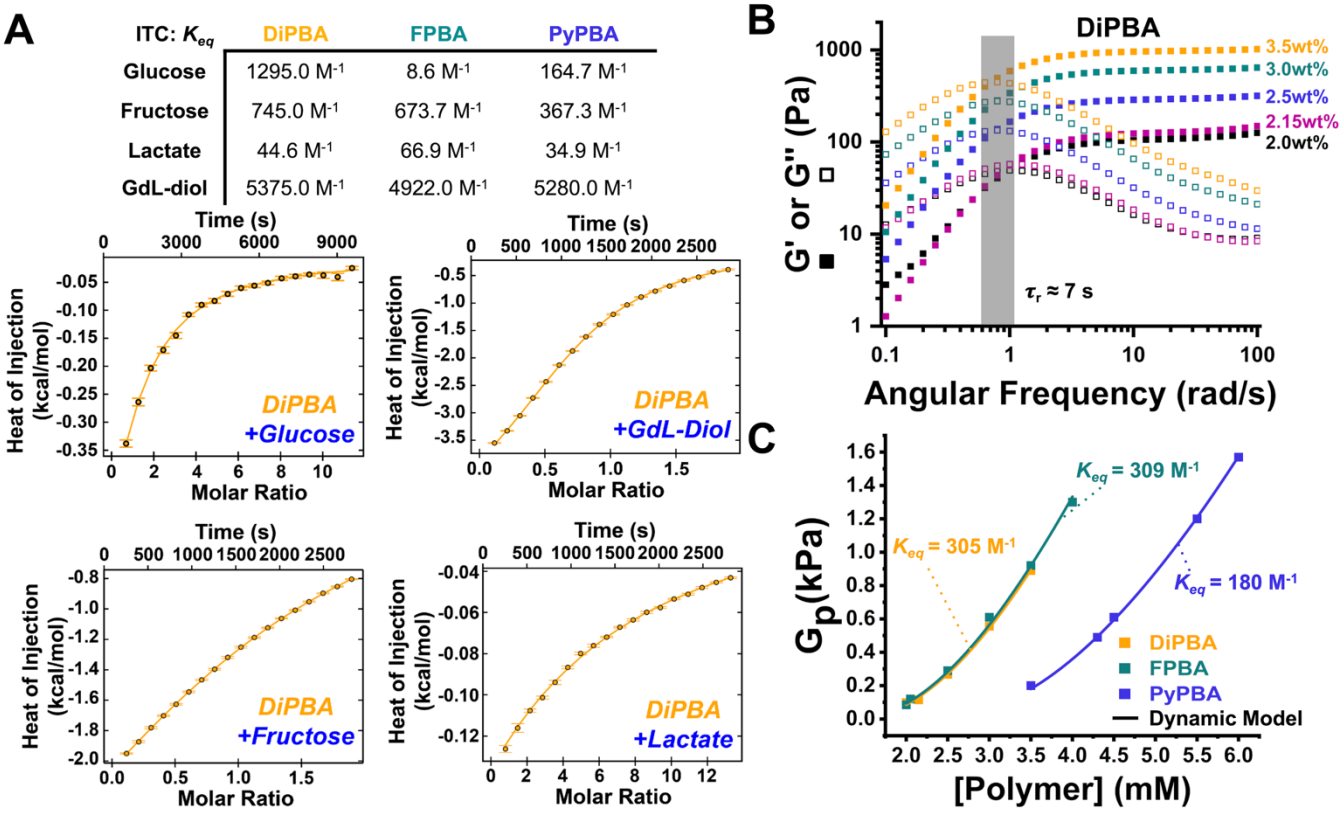

Figure 2: (**A**) Tabulated binding affinities (K_{eq}) determined from isothermal titration calorimetry (ITC) data performed on small molecule variants of the DiPBA, FPBA, and PyPBA binders with glucose, fructose, lactate, and a model diol crosslinker motif (GdL-diol) along with representative presentation of model-fitted data for DiPBA with each of these analytes. (**B**) Representative concentration-dependent oscillatory rheology frequency sweep data for hydrogels prepared from DiPBA–diol crosslinking. The G′/G″ crossover is used to approximate the network relaxation rate (τ_R). (**C**) The plateau moduli (G_p, G′ at twice G′/G″ crossover) from frequency sweeps of each network were fit to a dynamic-modified phantom network model to estimate the binding affinity (K_{eq}) of the dynamic-covalent crosslinking interactions in the gel.

exceeds the time constant of oscillation. In this regime, the behavior of materials scaled with frequency in a manner consistent with terminal relaxation and linear viscoelasticity ($G' \approx \omega^2$, $G'' \approx \omega'$).[35] PBA–diol dynamic-covalent crosslinking underlies the gelation behavior observed for these macromers; 5 wt% hydrogels prepared from equimolar mixing of DiPBA-4aPEG with Diol-4aPEG had a "zero-shear" viscosity of 133.5 kP and demonstrated shear-thinning behavior (***Fig S21***). By comparison, 5 wt% solutions of each macromer had viscosities roughly 6 orders of magnitude lower (~10 cP), no different from unmodified 4aPEG-OH. Accordingly, only in the presence of equimolar diPBA and diol groups did hydrogelation occur.

Using a dynamic-modified phantom network model developed for related PBA–diol ideal networks to establish the effective affinity of PBA–diol network crosslinking,[21] the K_{eq} of binding for different PBA-modified 4aPEGs to Diol-4aPEG was determined to be 305 M^{-1} (DiPBA), 309 M^{-1} (FPBA), and 180 M^{-1} (PyPBA) through model fitting (***Fig 2C***). The reader is encouraged to review the referenced work for specific details of this model.[21] Importantly, this model assumes ideal network behavior. Given canonical Maxwell behavior evident from terminal relaxation behavior and concentration-independent G′/G′′ crossover for the networks fit using this model herein, and by using simple 4aPEG precursors that yield a defined length of elastically active network strands, an ideal or "ideal-like" assumption is reasonable. Moreover, the macromers and crosslinking chemistries used here are, by design, very similar to those used to develop the model in this previous work. The possibility exists for some extent of non-ideality such as loops or entanglements,[36,37] though homogeneity in relaxation time across concentrations supports PBA–diol interactions as the dominant mode of network formation and dynamics. Reports on the overlap concentration (c*) of 4aPEG macromers in water—a good solvent for PEG when at near-ambient temperatures—further support limited entanglements in the concentration range of 2-6 wt% explored here.[38,39] Indeed, c* is estimated to be 11.5 wt% for these 10 kDa 4aPEG macromers, as calculated using reported methods (*see online supporting information*).[40,41] Accordingly, the combination of these factors support dynamic-covalent interactions between macromers as the primary contributor to network elasticity and validate selection of the dynamic-modified phantom network model to approximate K_{eq} for these networks.

The magnitude of K_{eq} values determined for the present materials are consistent with results from work that developed this dynamic-modified phantom network model, also using 4aPEG materials crosslinked by PBA–diol interactions (~275 M^{-1}).[21] Notably, the values derived when applying this model to the networks here were ~1 order of magnitude lower than those determined from ITC binding studies between small molecule PBAs and GdL-diol. This difference in binding affinity for motifs in the hydrogel state is perhaps reasonable given that presentation of multiple binding motifs on higher molecular weight macromers is expected to reduce the rate of association (k_{on}) as well as impose a relative penalty in translational entropy (ΔS) associated with linking large macromolecules as compared to interactions between small molecules. Indeed, when the DiPBA and GdL-diol motifs are presented on the ends of freely diffusing 5 kDa mPEG chains (***Fig S22***), a modest reduction in K_{eq} was observed for the interaction between these two motifs using ITC (~3×10^3 M^{-1}), with the interaction between the polymer-appended motifs being less entropically favorable ($\Delta S = 0.35$ cal/mol*K) compared to that between the small molecules ($\Delta S = 3.1$ cal/mol*K). In both cases, however, interactions are primarily enthalpically driven. Though these studies do not fully capture the differences observed once transitioned to use for hydrogel crosslinking on 4aPEG macromers, the combination of studies in ITC and rheology demonstrate the importance of characterizing interactions *in situ* and illustrate a key benefit of the dynamic-modified phantom network model to study this class of interactions. While all motifs bound GdL-diol comparably using ITC, in the gel state a small reduction in K_{eq} for PyPBA was observed relative to DiPBA and FPBA. This finding likewise demonstrates the importance of quantifying K_{eq} of dynamic-covalent crosslinking motifs *in situ* so as to reveal changes arising from polymer presentation of binding motifs.

The results for K_{eq} from this model, combined with k_{off} values estimated from G′/G′′ crossover values, enables approximation of k_{on} for DiPBA (42.7 $M^{-1}s^{-1}$), FPBA (139 $M^{-1}s^{-1}$), and PyPBA (41.4 $M^{-1}s^{-1}$) networks. These differences in association rates, especially between DiPBA and FPBA, may be attributed to different steric limitations of Diol binding for each PBA motif. As postulated initially from ITC results, similar association rates for DiPBA and PyPBA further support 1:1 binding stoichiometry between DiPBA and the GdL-derived diol used in network formation. These studies therefore illustrate comparable dynamic-covalent equilibrium bonding interactions for both DiPBA-4aPEG and FPBA-4aPEG to Diol-4aPEG, and while minor differences are apparent in the bond dynamics of these interactions their similar equilibrium binding state supports a focused comparison between this new DiPBA motif with the traditionally used FPBA motif for the remainder of the studies presented in this work.

Glucose-Responsive Gelation. Glucose-dependent dynamic material properties were next evaluated for these hydrogels using oscillatory rheology, comparing dynamic-covalent networks prepared from DiPBA–diol and FPBA–diol crosslinking. Hydrogels were formulated by mixing PBA-bearing 4aPEG macromers with equimolar Diol-4aPEG at a total polymer concentration of 2 mM (~2% w/v) in a pH 7.4 buffer containing various glucose concentrations (***Fig 3A***). As glucose concentration increased, it was hypothesized that hydrogels would become weaker due to increased competition from glucose with the underlying dynamic-covalent crosslinks. Since DiPBA binds with a higher affinity to glucose than does FPBA, it was also expected that DiPBA hydrogels would be more sensitive to glucose since the analyte would better compete for DiPBA crosslinks at comparable concentrations. Glucose concentrations were selected to span a physiologically relevant range from normoglycemic levels of 5.5 mM (100 mg/dL) to hyperglycemic levels of 22 mM (400 mg/dL). For ease in comparison, the G′ values were plotted for each glucose concentration at a frequency of 20 rad/s (***Fig 3B***); the same general trends hold for G′ over the apparent plateau region from 20-100 rad/s.–From this data, the DiPBA hydrogels demonstrated substantial reduction in their storage modulus with increased glucose. This result arises from an increased fraction of network crosslinks being disrupted, and thus less energy stored in the bonds of these networks under oscillatory deformation. At 22 mM glucose, the DiPBA network was no longer a self-supporting gel (***Fig S23***). The FPBA hydrogels, by comparison, exhibited some glucose-responsive change in storage modulus, though this effect was less dramatic than that observed for DiPBA; a stable hydrogel remained for FPBA in 22 mM glucose with only ~50% reduction in G′ compared to the glucose-free case. Accordingly, the DiPBA hydrogel platform affords more dramatic glucose-responsive mechanical properties at physiological glucose concentration. The underlying bond dynamics for the DiPBA hydrogels were likewise increased upon addition of glucose, with a shift in τ_R from 7 s (0 mM glucose) to 3 s (11 mM glucose). The increase in dynamics of network bonding is likewise expected due to increased competition from soluble glucose. In spite of glucose-responsive function being claimed in other reports of FPBA–diol hydrogels,[17] these studies did not conduct

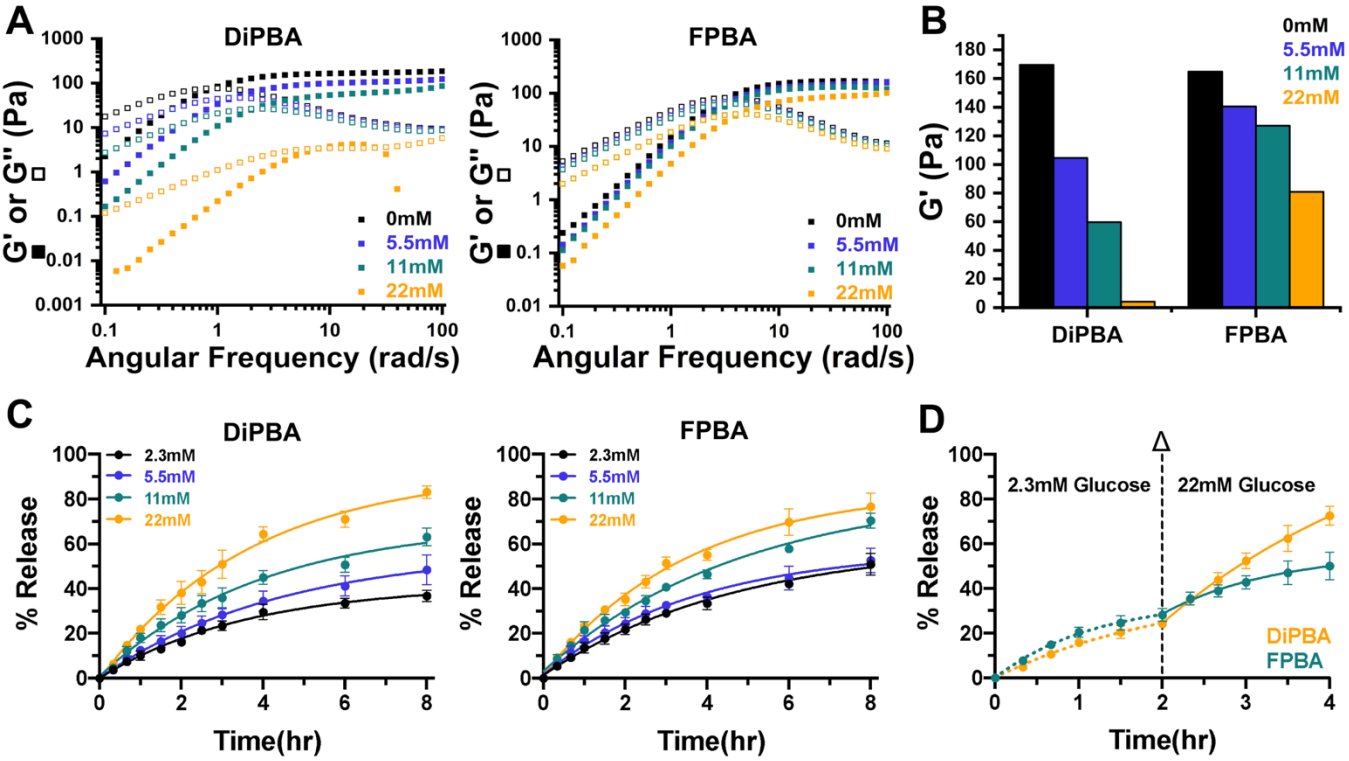

Figure 3: (**A**) Glucose-dependent oscillatory rheology frequency sweeps performed for networks crosslinked by DiPBA–Diol (*left*) or FPBA–Diol (*right*) dynamic-covalent interactions. Hydrogels were prepared at 2 mM macromer concentration in pH 7.4 buffer in all cases, with the addition of glucose at a concentration of 0, 5.5, 11, or 22 mM. (**B**) Comparative G' values (at 20 rad/s) for each hydrogel formulation at the various glucose concentrations. (**C**) Glucose-dependent release of FITC-insulin from hydrogels crosslinked by DiPBA–Diol (*left*) or FPBA–Diol (*right*) dynamic-covalent interactions. Hydrogels were prepared in a volume of 100 µL and 2 mM macromer concentration in 3.5 mL pH 7.4 buffer in all cases, with the addition of glucose in a bulk phase at concentrations of 2.3, 5.5, 11, or 22 mM. Data were fit to a standard first-order release model. (**D**) Step-change release, beginning with both DiPBA and FPBA hydrogels in a bulk glucose solution of 2.3 mM, with a complete exchange of the bulk buffer after 2 h to one containing 22 mM glucose. Data for each phase were fit to a standard first-order release model.

any glucose-dependent rheological measurements and thus comparison of the effect observed here to prior work is not possible.

Glucose-Responsive Insulin Release. After confirming glucose-responsive hydrogelation, controlled release of an encapsulated insulin payload was next assessed (***Fig 3C***). Hydrogels were prepared in all cases from a 1:1 molar ratio of the PBA or DiPBA motif to diol at 2 mM total macromer concentration in pH 7.4 buffer. As hydrogels were being formed, fluorescently labeled insulin was included for entrapment in the network to study its glucose-responsive release. Each hydrogel was immersed in a bulk buffer containing different physiologically relevant glucose concentrations ranging from 2.3 mM (42 mg/dL) to 22 mM (400 mg/dL). Significant glucose-dependent function was observed for the DiPBA hydrogel, evident in both its rate and amount of insulin release. Comparing the two glucose concentration extrema, the initial rate of release over the first 3 h increased from 0.08 h^{-1} (2.3 mM) to 0.20 h^{-1} (22 mM), while the total amount of insulin released at 8 h increased from 35% (2.3 mM) to 80% (22 mM). Though glucose-dependent differences were also evident in FPBA hydrogels, both the initial rate (0.10 h^{-1} vs. 0.16 h^{-1}) and final amount (50% vs. 75%) of insulin release were less dependent on glucose concentration (again, 2.3 mM vs. 22 mM). DiPBA hydrogels thus exhibit a release response directly dictated by glucose, whereas release from FPBA hydrogels is more modestly impacted. Some apparent disconnect between rheology data and release studies is evident; FPBA hydrogels had G′ values less impacted by glucose, yet both networks release insulin and FPBA actually releases more rapidly at lower glucose levels. It is important to note that the G′ values compared previously (***Fig 3B***) are dictated by K_{eq} of the network, yet network dynamics (*i.e.*, k_{on} and k_{off}) are also different between DiPBA and FPBA networks. With no glucose, the DiPBA networks are less dynamic than FPBA, but as glucose increases network dynamics of the DiPBA material increase rapidly. The mean mesh size of 4aPEG networks prepared from comparable molecular weight macromers at comparable weight percent was estimated as ~8 nm,[42] while insulin has a hydrodynamic diameter of ~6 nm nm in its most abundant zinc hexamer form.[43] Therefore, with some extent of obstruction-limited macromer solute diffusion, more rapid network dynamics likely yield higher effective diffusivity for insulin. Accordingly, release is accelerated in the FPBA networks without glucose, while the increased dynamics coupled with reduced crosslinking of the DiPBA network as glucose is increased likely underlie the significant acceleration in insulin release for this system. In addition, DiPBA hydrogel networks proved much more susceptible to erosion upon exposure to glucose than did FBPA networks (***Fig S24***), suggesting erosion-dominated release arising from glucose competing with PEG-appended diols to disrupt DiPBA network structure.

It is noted that prior work using 10 wt% FPBA–diol hydrogels showed very limited glucose-responsive release of insulin (~35 kDa as hexamer), though differences were observed for the release of a much larger IgG (~150 kDa) payload.[17] Glucose-responsive release of β-galactosidase (465 kDa) was also shown for a related PBA–diol network at 10 wt%.[19] Unlike these prior works, some glucose-responsive release of insulin was actually observed here using the FPBA–diol network, and this effect was improved using the DiPBA–diol network. It is hypothesized that this finding results from the lower polymer concentration (~2 wt%) used in these studies compared to prior work, improving the ability of glucose to compete with PEG-appended diols to shift the dynamic-covalent equilibrium and disrupt FPBA–diol crosslinking. To demonstrate this point, limited glucose-responsive function—as was previously reported for FPBA–diol hydrogels—was confirmed here for 10 wt% FPBA–diol hydrogels, whereas DiPBA–diol hydrogels maintained their glucose-responsive function at this elevated polymer concentration (***Fig S25***).

To improve function in blood glucose control, accelerated insulin release upon an increase in glucose level—as occurs following a meal—is a desirable property for a hydrogel depot. Accordingly, this function was assessed for hydrogels with encapsulated insulin by a sudden change in glucose concentration of the bulk release media (***Fig 3D***). Over an initial time of 2 h, gels were immersed in a release buffer containing 2.3 mM glucose. In this time, FPBA hydrogels released 30% of encapsulated insulin compared to 25% released from DiPBA hydrogels. After 2 h, the buffer was exchanged for a buffer containing 22 mM glucose to mimic a sudden increase in blood glucose. Over the ensuing 2 h, the total release for the FPBA hydrogels increased from 30% to 55%, while the DiPBA hydrogels showed a marked increase in release from 25% to 70%. These findings demonstrate increased responsiveness for the DiPBA platform, rapidly accelerating insulin release upon a sudden increase in glucose concentration.

Glucose-Specific Gelation. After establishing and comparing the relative glucose-responsive function of these hydrogels, their interaction with non-glucose analytes was next evaluated. Hydrogels were formulated at 2 mM (~2 wt%) macromer concentration, as before,

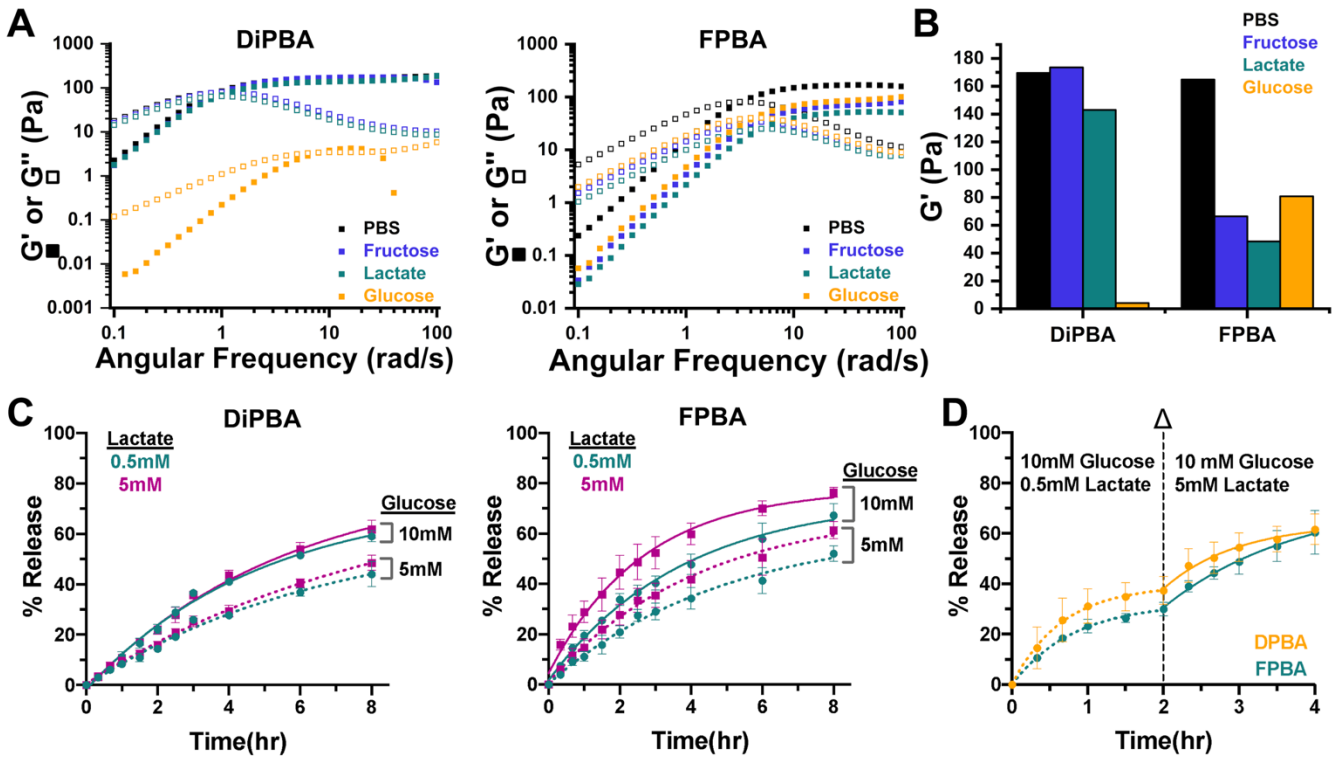

Figure 4: (**A**) Analyte-dependent oscillatory rheology frequency sweeps performed for networks crosslinked by DiPBA–Diol (*left*) or FPBA–Diol (*right*) dynamic-covalent interactions. Hydrogels were prepared at 2 mM macromer concentration in pH 7.4 buffer in all cases, with the addition of no analyte (PBS), fructose (1 mM), sodium lactate (5 mM), or glucose (22 mM). (**B**) G' (at 20 rad/s) for each hydrogel formulation when exposed to the various analytes. (**C**) Glucose- and lactate-dependent release of FITC-insulin from hydrogels crosslinked by DiPBA–Diol (*left*) or FPBA–Diol (*right*) dynamic-covalent interactions. Glucose concentration was either normal (5 mM, dashed) or moderately elevated (10 mM, solid), while lactate was either normal (0.5 mM, teal) or elevated (5 mM, magenta). Hydrogels were prepared in a volume of 100 μL and 2 mM macromer concentration in 3.5 mL pH 7.4 buffer in all cases, with the addition of glucose and lactate in the bulk phase at the concentrations indicated. Data were fit to a standard first-order release model. (**D**) Step-change release, beginning with both DiPBA and FPBA hydrogels in a bulk glucose solution of moderately elevated glucose (10 mM) and normal lactate (0.5 mM), with a complete exchange of the bulk buffer after 2 h to one containing the same glucose concentration (10 mM) but elevated lactate (5 mM). Data for each phase were fit to a standard first-order release model.

with different amounts of competing analytes. From the initial ITC results, it was hypothesized that the DiPBA hydrogel should be less sensitive to crosslink disruption by non-glucose analytes than would the FPBA hydrogel. The concentrations of the competing analytes studied were 1 mM for fructose and 5 mM for lactate, selected to be on the upper end of their physiologically relevant range of exposure.[44,45] These results were compared to the hydrogel response resulting from incubation with 22 mM glucose, also on its upper end of diabetic physiological exposure concentration. Oscillatory rheology was performed as before (***Fig 4A***), and G′ values were compared as described before for each hydrogel formulation with each analyte (***Fig 4B***). These results point to limited responsiveness of the DiPBA hydrogel to 5 mM lactate (G′ = 143 Pa) and 1 mM fructose (G′ = 174 Pa) compared to 22 mM glucose (G′ = 4 Pa~~, *sol*~~). These data thus support the glucose specificity of DiPBA crosslinking chemistry relative to its response to non-glucose analytes present at their physiological concentrations. The FPBA hydrogel, by comparison, responded comparably to lactate (G′ = 48 Pa) and fructose (G′ = 66 Pa) as it did to glucose (G′ = 81 Pa), indicating no glucose specificity of the crosslinking mechanism in this platform. Though ITC data suggested similar affinities for both DiPBA and FPBA binding to fructose and lactate, the results evident from the impact of these analytes on gelation offer a striking contrast. As ITC only captures the equilibrium state, rheological differences could arise from the difference network dynamics previously described, wherein the more dynamic FPBA hydrogel rendered it more susceptible to competition from analytes. Again, this discrepancy points to the importance of evaluating molecular-scale crosslinking interactions *in situ*.

Glucose-Specific Insulin Release. In the context of insulin therapy, interference from lactate presents an especially problematic outcome for a delivery depot; whereas fructose arises from dietary sources and typically overlaps with glucose consumption and insulin

need,[46] lactate is frequently elevated during and after periods of vigorous exercise.[47] Lactate is also known to be elevated in diabetics with poorly managed disease.[48,49] Thus, the impact of lactate was further explored for its role in triggering undesired insulin release from PBA–diol hydrogels (***Fig 4C***). DiPBA-4aPEG or FPBA-4aPEG macromers were mixed with equimolar Diol-4aPEG at 2 mM total macromer concentration and incubated in a buffer containing physiologically relevant glucose and lactate concentrations. Four conditions were selected, combining glucose that was either normal (5 mM) or slightly elevated (10 mM) with physiologically relevant lactate levels mimicking normal (0.5 mM) and elevated (5 mM) states. The presence of lactate prompted no significant enhancement in insulin release from DiPBA hydrogels; these instead had release profiles that were fully dictated by glucose level but independent of the addition of either normal or high levels of lactate. The FPBA hydrogels, conversely, showed increased release in response to increases in both glucose and lactate. These findings corroborate data demonstrated previously in both ITC and rheology studies that showed FPBA–lactate binding and lactate-driven network disruption, respectively.

As lactate levels may rise quickly with vigorous exercise, this scenario was recreated by studying the change in insulin release upon a sudden change in a stable environment of slightly elevated glucose (10 mM) from low (0.5 mM) to high (5 mM) lactate levels (***Fig 4D***). Hydrogels were immersed in a buffer containing 10 mM glucose and 0.5 mM lactate for an initial period of 2 h. Over this time, FPBA hydrogels released 30% of their insulin while DiPBA released 35%, confirming the increased glucose-responsiveness of the DiPBA platform observed previously at moderately elevated glucose. After this initial period, the buffer was then exchanged for a buffer that maintained the 10 mM glucose concentration but increased lactate levels to 5 mM. Over this additional 2 h period at elevated lactate, FPBA hydrogels released an additional 40% of encapsulated insulin, while DiPBA hydrogels released only an additional 25% of encapsulated insulin. These data further support the non-specific sensitivity of FPBA hydrogels, whereas release from DiPBA hydrogels was not substantially impacted by elevated lactate as a model physiologically relevant non-glucose analyte.

Responsive Therapeutic Function. In order to verify therapeutic function of this DiPBA-based hydrogel platform, an *in vivo* study in streptozotocin-induced diabetic mice was performed (***Fig 5A***). This model recreates pathological features of Type-1 diabetes through chemical destruction of pancreatic β-cells, leading to a hyperglycemic and insulin-deficient phenotype. Fasted mice that remained in a state of severe hyperglycemia (>550 mg/dL) were subcutaneously administered DiPBA or FPBA hydrogels with encapsulated insulin, alongside controls of free insulin and saline. Insulin dosing was selected for matched potency upon initial administration, evident in the rate of blood glucose reduction, while simultaneously avoiding incidence of overdose leading to severe hypoglycemia (<50 mg.dL); thus 4 IU/kg was administered for insulin alone and 7 IU/kg administered for insulin encapsulated in hydrogels. Glucose levels were monitored over time using handheld glucometers (***Fig 5B***). Treatment with both DiPBA and FPBA hydrogels, as well as that with control insulin, demonstrated blood glucose correction following administration; hydrogels reduced blood glucose to ~60-80 mg/dL and insulin reduced blood glucose to ~100 mg/dL. Differences in both the onset and duration of action between the free insulin control and both hydrogels were evident in this early time, with insulin reaching its nadir value at ~1 h and slowly increasing after this time while both hydrogels continued to reduce blood glucose levels to achieve nadir at ~3 h; this corresponds to the expected controlled release of insulin from hydrogels. Saline treatment, meanwhile, demonstrated some blood glucose reduction expected due to continued fasting and recovery from the stimulation of handling and injection. A key objective of these studies was to determine the relative responsiveness of DiPBA–diol networks compared to those prepared using FPBA–diol. As such, following administration and blood glucose correction an intraperitoneal glucose tolerance test (GTT) was performed on all mice. Both hydrogels demonstrated blood glucose recovery approaching their pre-challenge baseline over 3 h, while insulin treated mice had dramatically increased blood glucose without any subsequent correction. This cycle was repeated a second time, where DiPBA and FPBA hydrogels again demonstrated blood glucose correction. Comparing the area under the curve (AUC) following each challenge, the DiPBA hydrogels exhibited significantly improved responsiveness ($P<0.05$) when compared to FPBA hydrogels following both rounds of GTT (***Fig 5C***). This effect is especially evident in the second challenge, where AUC values were doubled for FPBA-treated mice compared to DiPBA treatment. The FPBA hydrogels also failed to correct blood glucose back to a normoglycemic range for mice (BG ≤180 mg/dL) within 3 h of the second GTT. The improved responsiveness exhibited by DiPBA hydrogels is attributed to its more sensitive and glucose-specific mode of release. At the time of the second challenge, there is less insulin on board hydrogels due to 6 h of prior release. Accordingly, the more rapid

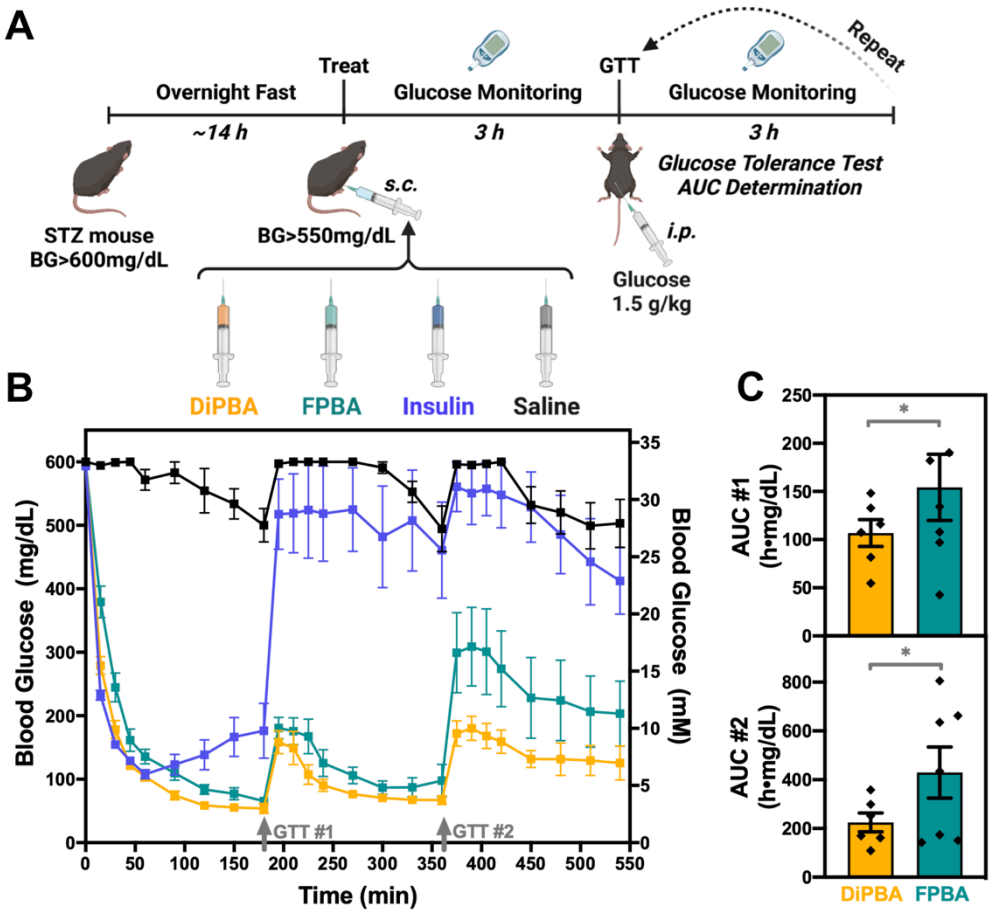

Figure 5: (**A**) A schematic overview with of the experimental procedure to assess *in vivo* the glucose-responsive function of hydrogels, evaluating these in streptozotocin (STZ)-induced diabetic mice with multiple intraperitoneal glucose tolerance tests (GTT). (**B**) Blood glucose monitoring following therapeutic administration (t=0), including two glucose tolerance tests (t=180 and 360 minutes). Mice were randomized into treatment groups with n=6-7 per group. (**C**) The area under the curve (AUC) following each GTT was quantified by the trapezoidal method and compared for the two hydrogel formulations, with significance (*- P<0.05) determined using Student's t-test.

responsiveness demonstrated *in vitro* (***Fig 3D***) likely enables increased release of remaining depleted insulin reserve from DiPBA hydrogels in response to the second GTT. Unfortunately, the dynamic and deformable nature of the hydrogels made impossible any post-mortem isolation to quantify insulin remaining in the hydrogels at the study endpoint. It is also not possible to place these results in the context of other work on PBA–diol hydrogels, as these prior technologies were not evaluated in a therapeutic capacity *in vivo*.

CONCLUSIONS

Diborantes have been explored as molecular glucose sensors for their ability to bind glucose at physiologically relevant concentrations and their resistance to interference by non-glucose analytes. Herein, a new DiPBA motif was developed and used for the first time to prepare dynamic-covalent hydrogels networks. Molecular-scale binding studies using ITC demonstrated this new DiPBA to have glucose affinity that was 150 times higher than that of a traditional PBA motif. Simultaneously, this DiPBA motif showed reduced binding to fructose and lactate; interference from these non-glucose analytes presents a significant hurdle to the use of PBA-based materials due to the possibility that these physiological analytes, and specifically lactate, may trigger non-specific insulin release. Rheology studies on dynamic-covalent hydrogels demonstrated DiPBA–diol crosslinking to be more glucose-sensitive than FPBA–diol crosslinking. In addition, hydrogels crosslinked by DiPBA–diol interactions were minimally impacted by non-glucose analytes like fructose and lactate; these analytes were at least as effective as glucose in disrupting crosslinking of FPBA–diol materials. In the context of glucose-responsive insulin delivery for blood glucose management in diabetes, the glucose sensing and specificity of DiPBA–diol crosslinking translated to improved glucose-responsive insulin release from the hydrogels. The improved responsiveness of DiPBA-based

crosslinking was further validated in a diabetic mouse model, exhibiting more effective blood glucose correction following multiple glucose challenges. This approach to use more sensitive and specific DiPBA–diol crosslinking thus offers a new material-centered approach with the potential to achieve the longstanding goal of glucose-responsive insulin therapy, overcoming limitations of commonly used PBA-based crosslinking chemistries.

EXPERIMENTAL PROCEDURES

Synthetic Methods. For detailed synthetic schemes and methodology, as well as ^{1}H NMR characterization, please see the online supporting information.

Acid-Base Titration. In order to determine pK_a for the small molecule boronate variants used here, a 0.01 M stock solution of the PBA of interest was prepared by dissolving 0.2 mmol of each PBA in 20 mL DI water. The solution was then titrated with 0.005 M NaOH solution under constant stirring with pH monitoring.

Isothermal Titration Calorimetry. The binding affinities (K_{eq}) between different small molecule PBAs and model analytes (***Fig S3***) were measured through isothermal titration calorimetry (ITC). All titration experiments were performed at 298 K on a PEAQ-ITC calorimeter (MicroCal, Inc.) in degassed pH 7.4 PBS buffer, using a 38 µL syringe and 200 µL cells and consisting of 19 injections. The measurements were performed by titrating glucose, fructose, sodium lactate or $Diol_{sm}$ from the syringe into a solution of small molecule variants of $DiPBA_{sm}$, $PyPBA_{sm}$, or $FPBA_{sm}$ loaded in the cell. In all titration experiments, the cell concentration was 1mM, while the analyte concentrations in the syringe were varied according to experimental optimization. All raw data were corrected by subtraction of a dilution measurement of the titrated analytes into buffer, and were then analyzed and graphed using the integrated public-domain software packages of NIPIC, SEDPHAT, and GUSSI according to a published protocol.[50]

Oscillatory Rheology. Hydrogel mechanical properties were evaluated with a TA Instruments HR-2 rheometer fitted with a Peltier stage set to 25^{o}C. All measurements were performed using a 25 mm parallel plate geometry. Oscillatory strain amplitude sweep measurements were first conducted at a frequency of 20 rad/s. Oscillatory frequency sweep measurements were then conducted at 3% strain after verification that this was in the linear viscoelastic region for all materials. Several rheology studies were performed, and hydrogels were prepared according to the various parameters being assessed: ***i)*** For studies of concentration-dependent hydrogelation, stock solutions of PBA-bearing macromers (DiPBA-4aPEG, PyPBA-4aPEG, or FPBA-4aPEG) and Diol-4aPEG were prepared in 1X PBS. To formulate hydrogels, appropriate volumes of each macomer stock solution (*at 1:1 motif to diol by mole*) and PBS were combined to yield the final desired polymer concentration. ***ii)*** For studies of glucose-dependent hydrogelation, glucose-containing buffers were prepared by dissolving glucose with PBS to yield a desired glucose concentration (0 mg/dL, 100 mg/dL, 200 mg/dL, and 400 mg/dL). Then stock solutions of PBA-bearing macromers (DiPBA-4aPEG, PyPBA-4aPEG, or FPBA-4aPEG) and Diol-4aPEG were prepared in these various glucose-containing PBS solutions. To formulate hydrogels, appropriate volumes of each macomer stock solution (*at 1:1 motif to diol by mole*) were combined to yield a final desired polymer concentration of 2 mM. ***iii)*** For analyte-dependent hydrogelation, lactate, fructose, and glucose were dissolved in PBS to yield their final desired concentrations (Lactate: 5 mM, Fructose: 1 mM, Glucose: 22 mM). Then stock solutions of PBA-bearing macromers (DiPBA-4aPEG, PyPBA-4aPEG, or FPBA-4aPEG) and Diol-4aPEG were prepared in these various PBS solutions. To formulate the hydrogels, appropriate volumes of each macomer stock solution (*at 1:1 motif to diol by mole*) were combined to yield a final desired polymer concentration of 2 mM in the buffer containing the desired analyte.

FITC-insulin release studies. A variety of studies were performed to assess the glucose-responsive and glucose-specific release of insulin from hydrogels. ***i)*** To evaluate glucose-dependent FITC-insulin release from hydrogels, 0.1 ml hydrogels were prepared in a pH 7.4 PBS buffer at 2 mM polymer concentration (*at 1:1 motif to diol by mole*) along with 20 µg FITC-insulin per hydrogel. Gels were then incubated in circular molds placed within 12-well plates and immersed in 3.5 mL of pH 7.4 release buffer containing 2.3, 5.5, 11 or 22 mM of glucose. At each time point, a 20 µL aliquot was taken and further diluted to 200 µL for fluorescence analysis (Ex: 485 nm, Em: 520 nm) on a Tecan M200 plate reader. The bulk was adjusted by addition of 20 µL of the same release buffer to maintain constant volume with each sampling. Released FITC-insulin concentrations were determined using a standard curve. After 8 h, gels were manually destroyed by treating with HCl solution to disrupt any remaining gel network and free residual FITC-insulin. The pH of this mixture was adjusted to pH 7.4 and insulin was quantified for mass balance closure. ***ii)*** To evaluate FITC-insulin release upon a sudden increase in glucose level to mimic a hyperglycemic spike, hydrogels were prepared as before and immersed in 3.5 mL of pH 7.4 release buffer containing 2.3 mM glucose for 2 h. Subsequently, the release buffer was completely removed and replaced with 3.5 mL of pH 7.4 buffer containing 22 mM glucose and

release was monitored for an additional 2 h. At each time point, a 20 μL aliquot was taken and further diluted to 200 μL for fluorescence analysis, and endpoint analysis and mass balance closure were performed, as before. ***iii)*** To evaluate glucose-specific FITC-insulin release from hydrogels, 0.1 ml of hydrogel were prepared as before in pH 7.4 PBS at 2 mM polymer concentration and containing 20 μg FITC-insulin. Gels were then immersed in 3.5 mL of pH 7.4 PBS containing either *a)* 5 mM glucose and 0.5 mM sodium lactate, *b)* 5 mM glucose and 5 mM sodium lactate, *c)* 10mM glucose and 0.5mM sodium lactate, or *d)* 10mM glucose and 5mM sodium lactate. At each time point, 20 μL samples were collected, diluted to 200 μL, and analyzed as normal, along with replacement of 20 μL fresh buffer to the bulk. After 8 hours, gels were manually destroyed by HCl and analyzed for insulin content to ensure mass balance closure. ***iv)*** To evaluate FITC-insulin release with a sudden increase in sodium lactate to mimic post-exercise elevation, 0.1 ml of hydrogel were prepared as before in pH 7.4 PBS at 2 mM polymer concentration and containing 20 μg FITC-insulin. Gels were then immersed in 3.5 mL of pH 7.4 buffer containing 10 mM glucose and 0.5 mM sodium lactate for 2 h. Subsequently, the release buffer was completely removed and replaced with 3.5 mL of pH 7.4 buffer containing 10 mM glucose and 5 mM sodium lactate for 2 h. At each time point, a 20 μL aliquot was taken and further diluted to 200 μL for fluorescence analysis, and endpoint analysis and mass balance closure were performed, as before.

Blood glucose control *in vivo*. To evaluate the performance hydrogels for blood glucose control, male C57BL6/J mice (8 weeks old, ~25 g/mouse; Jackson Laboratory) were induced to be insulin deficient using streptozotocin (STZ). Mice were fasted for 4 h, following which a single intraperitoneal (i.p.) injection of STZ at a dose of 150 mg/kg was administered. Following an additional 30 min fast, food was returned. Seven days following STZ treatment, insulin-deficient diabetes was verified using hand-held blood glucose meters (CVS brand) with unfasted blood glucose (BG) levels ensured to be above 600 mg/dL for study inclusion. Mice were then fasted for 12 h, and those with BG > 550 mg/dL were randomly divided into 4 groups (n=6-7/group). Groups were treated with one of the following: *a)* 0.1 mL pH 7.4 PBS buffer, *b)* 0.1 mL human recombinant insulin (4 IU/kg), *c)* 0.1 mL insulin-loaded DiPBA hydrogel (1:1 molar ratio of DiPBA-4aPEG to Diol-4aPEG, insulin dose of 7 IU/kg), or *d)* 0.1 mL insulin-loaded FPBA hydrogel (1:1 molar ratio of FPBA-4aPEG to Diol-4aPEG, insulin dose of 7 IU/kg) *via* subcutaneous (s.c.) injection. BG level were continuously monitored for 3 h after treatment. To examine gel response to a sudden increase in BG, a glucose tolerance test was performed by i.p. injection of glucose (1.25 g/kg glucose, 0.1 mL). BG were subsequently monitored for 3 h. A total of two IPGTT cycles were performed. Mice were fasted for the duration of the experiment with continuous access to water. All experiments followed a protocol (#21-11-6916) approved by the University of Notre Dame Animal Care and Use Committee (IACUC) and adhered to all relevant Institutional, State, and Federal guidelines. Area under the curve (AUC) was calculated using the trapezoidal rule and statistical analysis was performed to compare DiPBA and FPBA treatment groups using Graphpad Prism v9.0, with significance obtained using a Student's t-test.

SUPPLEMENTAL INFORMATION DESCRIPTION

The Online Supporting Information (.PDF) includes: Detailed synthetic methods, schemes, and ^{1}H NMR characterization data; Acid-Base Titration; Isothermal Titration Calorimetry (ITC); ESI-MS; Rheology; Release Study.

ACKNOWLEDGMENTS

MJW gratefully acknowledges funding support for this work from the Juvenile Diabetes Research Foundation (5-CDA-2020-947-A-N), the Helmsley Charitable Trust (grants 2019PG-T1D016 and 2102-04994), the American Diabetes Association Pathway Accelerator Award (1-19-ACE-31), and a National Science Foundation CAREER award (BMAT, 1944875). Schematics in TOC artwork, Fig 1, and Fig 5 created using BioRender.com.

AUTHOR CONTRIBUTIONS

YX and SX contributed equally to this work. YX, SX, and MJW conceived of ideas, designed/conducted experiments, analyzed data, and wrote the manuscript. SY, BS, and IP contributed to experiments and data collection.

DECLARATION OF INTEREST

The authors declare no competing interests.

REFERENCES

[1] N.A. Peppas, Y. Huang, M. Torres-Lugo, J.H. Ward, J. Zhang, Physicochemical Foundations and Structural Design of Hydrogels in Medicine and Biology, Annual Review of Biomedical Engineering. 2 (2000) 9–29. https://doi.org/10.1146/annurev.bioeng.2.1.9.

[2] J.L. Drury, D.J. Mooney, Hydrogels for tissue engineering: scaffold design variables and applications, Biomaterials. 24 (2003) 4337–4351. https://doi.org/10.1016/s0142-9612(03)00340-5.

[3] M. Guvendiren, H.D. Lu, J.A. Burdick, Shear-thinning

hydrogels for biomedical applications, Soft Matter. 8 (2012) 260–272. https://doi.org/10.1039/c1sm06513k.
[4] J. Li, D.J. Mooney, Designing hydrogels for controlled drug delivery, Nature Reviews Materials. 1 (2016). https://doi.org/10.1038/natrevmats.2016.71.
[5] M.J. Webber, E.T. Pashuck, (Macro)molecular self-assembly for hydrogel drug delivery, Adv. Drug Deliv. Rev. 172 (2021) 275–295.
[6] J.K. Sahoo, M.A. VandenBerg, M.J. Webber, Injectable network biomaterials via molecular or colloidal self-assembly, Adv. Drug Deliv. Rev. 127 (2018) 185–207.
[7] A.S. Hoffman, Hydrogels for biomedical applications, Adv. Drug Deliv. Rev. 54 (2002) 3–12.
[8] S.M. Mantooth, B.G. Munoz-Robles, M.J. Webber, Dynamic Hydrogels from Host-Guest Supramolecular Interactions, Macromol. Biosci. 19 (2019) e1800281.
[9] W.E. Hennink, C.F. van Nostrum, Novel crosslinking methods to design hydrogels, Advanced Drug Delivery Reviews. 64 (2012) 223–236. https://doi.org/10.1016/j.addr.2012.09.009.
[10] S.J. Rowan, S.J. Cantrill, G.R.L. Cousins, J.K.M. Sanders, J.F. Stoddart, Dynamic covalent chemistry, Angew. Chem. Int. Ed Engl. 41 (2002) 898–952.
[11] Y. Jin, C. Yu, R.J. Denman, W. Zhang, Recent advances in dynamic covalent chemistry, Chemical Society Reviews. 42 (2013) 6634. https://doi.org/10.1039/c3cs60044k.
[12] S. Tang, B.M. Richardson, K.S. Anseth, Dynamic covalent hydrogels as biomaterials to mimic the viscoelasticity of soft tissues, Progress in Materials Science. 120 (2021) 100738. https://doi.org/10.1016/j.pmatsci.2020.100738.
[13] A.M. Rosales, K.S. Anseth, The design of reversible hydrogels to capture extracellular matrix dynamics, Nat Rev Mater. 1 (2016). https://doi.org/10.1038/natrevmats.2015.12.
[14] M.J. Webber, M.W. Tibbitt, Dynamic and reconfigurable materials from reversible network interactions, Nature Reviews Materials. (2022). https://doi.org/10.1038/s41578-021-00412-x.
[15] W.L.A. Brooks, B.S. Sumerlin, Synthesis and Applications of Boronic Acid-Containing Polymers: From Materials to Medicine, Chem. Rev. 116 (2016) 1375–1397.
[16] M.A. VandenBerg, M.J. Webber, Biologically Inspired and Chemically Derived Methods for Glucose-Responsive Insulin Therapy, Adv. Healthc. Mater. 8 (2019) e1801466.
[17] V. Yesilyurt, M.J. Webber, E.A. Appel, C. Godwin, R. Langer, D.G. Anderson, Injectable Self-Healing Glucose-Responsive Hydrogels with pH-Regulated Mechanical Properties, Adv. Mater. 28 (2016) 86–91.
[18] Y. Dong, W. Wang, O. Veiseh, E.A. Appel, K. Xue, M.J. Webber, B.C. Tang, X.-W. Yang, G.C. Weir, R. Langer, D.G. Anderson, Injectable and Glucose-Responsive Hydrogels Based on Boronic Acid-Glucose Complexation, Langmuir. 32 (2016) 8743–8747.
[19] B. Marco-Dufort, J. Willi, F. Vielba-Gomez, F. Gatti, M.W. Tibbitt, Environment Controls Biomolecule Release from Dynamic Covalent Hydrogels, Biomacromolecules. 22 (2021) 146–157.
[20] C.C. Deng, W.L.A. Brooks, K.A. Abboud, B.S. Sumerlin, Boronic Acid-Based Hydrogels Undergo Self-Healing at Neutral and Acidic pH, ACS Macro Letters. 4 (2015) 220–224. https://doi.org/10.1021/acsmacrolett.5b00018.
[21] B. Marco-Dufort, R. Iten, M.W. Tibbitt, Linking Molecular Behavior to Macroscopic Properties in Ideal Dynamic Covalent Networks, J. Am. Chem. Soc. 142 (2020) 15371–15385.
[22] G. Springsteen, B. Wang, A detailed examination of boronic acid–diol complexation, Tetrahedron. 58 (2002) 5291–5300.
[23] S. Friedman, B. Pace, R. Pizer, Complexation of phenylboronic acid with lactic acid. Stability constant and reaction kinetics, Journal of the American Chemical Society. 96 (1974) 5381–5384. https://doi.org/10.1021/ja00824a012.
[24] B. Wang, K.-H. Chou, B.N. Queenan, S. Pennathur, G.C. Bazan, Molecular Design of a New Diboronic Acid for the Electrohydrodynamic Monitoring of Glucose, Angew. Chem. Int. Ed Engl. 58 (2019) 10612–10615.
[25] Z. Guo, I. Shin, J. Yoon, Recognition and sensing of various species using boronic acid derivatives, Chem. Commun. . 48 (2012) 5956–5967.
[26] W. Yang, H. He, D.G. Drueckhammer, Computer-Guided Design in Molecular Recognition: Design and Synthesis of a Glucopyranose Receptor, Angewandte Chemie. 113 (2001) 1764–1768. https://doi.org/10.1002/1521-3757(20010504)113:9<1764::aid-ange17640>3.0.co;2-y.
[27] T.D. James, K.R. Samankumara Sandanayake, S. Shinkai, A Glucose-Selective Molecular Fluorescence Sensor, Angewandte Chemie International Edition in English. 33 (1994) 2207–2209. https://doi.org/10.1002/anie.199422071.
[28] H. Eggert, J. Frederiksen, C. Morin, J.C. Norrild, A New Glucose-Selective Fluorescent Bisboronic Acid. First Report of Strong α-Furanose Complexation in Aqueous Solution at Physiological pH[1], The Journal of Organic Chemistry. 64 (1999) 3846–3852. https://doi.org/10.1021/jo9819279.
[29] X. Sun, T.D. James, Glucose Sensing in Supramolecular Chemistry, Chem. Rev. 115 (2015) 8001–8037.
[30] D.H.-C. Chou, M.J. Webber, B.C. Tang, A.B. Lin, L.S. Thapa, D. Deng, J.V. Truong, A.B. Cortinas, R. Langer, D.G. Anderson, Glucose-responsive insulin activity by covalent modification with aliphatic phenylboronic acid conjugates, Proc. Natl. Acad. Sci. U. S. A. 112 (2015) 2401–2406.
[31] A. Matsumoto, T. Ishii, J. Nishida, H. Matsumoto, K. Kataoka, Y. Miyahara, A Synthetic Approach Toward a Self-Regulated Insulin Delivery System, Angewandte Chemie. 124 (2012) 2166–2170. https://doi.org/10.1002/ange.201106252.
[32] L.K. Mohler, A.W. Czarnik, Ribonucleoside membrane transport by a new class of synthetic carrier, Journal of the American Chemical Society. 115 (1993) 2998–2999. https://doi.org/10.1021/ja00060a067.
[33] W.C. Yount, D.M. Loveless, S.L. Craig, Small-molecule dynamics and mechanisms underlying the macroscopic mechanical properties of coordinatively cross-linked polymer networks, J. Am. Chem. Soc. 127 (2005) 14488–14496.
[34] L. Zou, A.S. Braegelman, M.J. Webber, Dynamic Supramolecular Hydrogels Spanning an Unprecedented Range of Host–Guest Affinity, ACS Applied Materials & Interfaces. 11 (2019) 5695–5700. https://doi.org/10.1021/acsami.8b22151.
[35] T. FitzSimons, F. Oentoro, T.V. Shanbhag, E. Anslyn, A. Rosales, Preferential Control of Forward Reaction Kinetics in Hydrogels Crosslinked with Reversible Conjugate Additions, (n.d.). https://doi.org/10.26434/chemrxiv.11823684.
[36] M. Shibayama, Spatial inhomogeneity and dynamic fluctuations of polymer gels, Macromolecular Chemistry and Physics. 199 (1998) 1–30. https://doi.org/10.1002/(sici)1521-3935(19980101)199:1<1::aid-macp1>3.0.co;2-m.
[37] F.D. Lorenzo, F. Di Lorenzo, S. Seiffert, Nanostructural heterogeneity in polymer networks and gels, Polymer Chemistry. 6 (2015) 5515–5528. https://doi.org/10.1039/c4py01677g.
[38] M.D. Wehrman, A. Leduc, H.E. Callahan, M.S. Mazzeo, M. Schumm, K.M. Schultz, Rheological properties and structure of step- and chain-growth gels concentrated above the overlap concentration, AIChE Journal. 64 (2018) 3168–3176.

https://doi.org/10.1002/aic.16062.
[39] W. Liu, X. Gong, Y. Zhu, J. Wang, T. Ngai, C. Wu, Probing Sol–Gel Matrices and Dynamics of Star PEG Hydrogels Near Overlap Concentration, Macromolecules. 52 (2019) 8956–8966. https://doi.org/10.1021/acs.macromol.9b01489.
[40] H. Zhang, M.D. Wehrman, K.M. Schultz, Structural Changes in Polymeric Gel Scaffolds Around the Overlap Concentration, Front Chem. 7 (2019) 317.
[41] K. Devanand, J.C. Selser, Asymptotic behavior and long-range interactions in aqueous solutions of poly(ethylene oxide), Macromolecules. 24 (1991) 5943–5947. https://doi.org/10.1021/ma00022a008.
[42] S.T. Lust, D. Hoogland, M.D.A. Norman, C. Kerins, J. Omar, G.M. Jowett, T.T.L. Yu, Z. Yan, J.Z. Xu, D. Marciano, R.M.P. da Silva, C.A. Dreiss, P. Lamata, R.J. Shipley, E. Gentleman, Selectively Cross-Linked Tetra-PEG Hydrogels Provide Control over Mechanical Strength with Minimal Impact on Diffusivity, ACS Biomater Sci Eng. 7 (2021) 4293–4304.
[43] S.S. Jensen, H. Jensen, C. Cornett, E.H. Møller, J. Østergaard, Insulin diffusion and self-association characterized by real-time UV imaging and Taylor dispersion analysis, J. Pharm. Biomed. Anal. 92 (2014) 203–210.
[44] S.A. Hannou, D.E. Haslam, N.M. McKeown, M.A. Herman, Fructose metabolism and metabolic disease, J. Clin. Invest. 128 (2018) 545–555.
[45] B. Phypers, J.M.T. Pierce, Lactate physiology in health and disease, Contin Educ Anaesth Crit Care Pain. 6 (2006) 128–132.
[46] K.L. Stanhope, P.J. Havel, Fructose consumption: recent results and their potential implications, Ann. N. Y. Acad. Sci. 1190 (2010) 15–24.
[47] T.T. Gleeson, Post-exercise lactate metabolism: a comparative review of sites, pathways, and regulation, Annu. Rev. Physiol. 58 (1996) 565–581.
[48] M.M. Christopher, J.D. Broussard, C.W. Fallin, N.J. Drost, M.E. Peterson, Increased serum D-lactate associated with diabetic ketoacidosis, Metabolism. 44 (1995) 287–290.
[49] L.W. Andersen, J. Mackenhauer, J.C. Roberts, K.M. Berg, M.N. Cocchi, M.W. Donnino, Etiology and therapeutic approach to elevated lactate levels, Mayo Clin. Proc. 88 (2013) 1127–1140.
[50] C.A. Brautigam, H. Zhao, C. Vargas, S. Keller, P. Schuck, Integration and global analysis of isothermal titration calorimetry data for studying macromolecular interactions, Nat. Protoc. 11 (2016) 882–894.

Graphical Abstract:

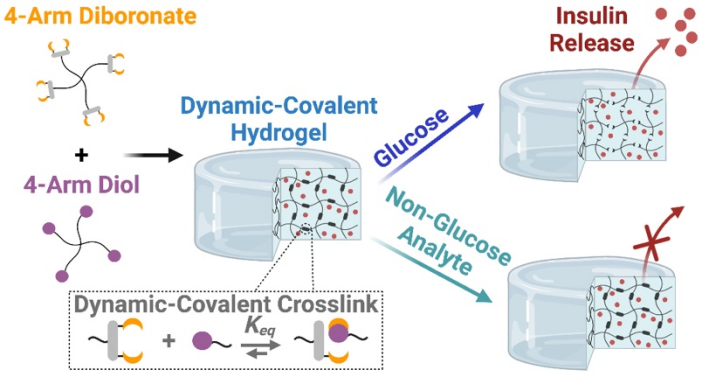

Caption:

The preparation of hydrogels crosslinked using diboronate motifs affords more glucose-specific and glucose-responsive function compared to traditional routes based on phenylboronic acid that suffer from interference by non-glucose analytes.